

**THE EFFECT OF TWO LATERAL INFLOW CHANNELS ON MAIN
CHANNEL DISCHARGE**

BY

CHIRCHIR CHERUIYOT AMOS

**A THESIS SUBMITTED IN PARTIAL FULFILLMENT OF THE
REQUIREMENTS FOR THE DEGREE OF MASTER OF SCIENCE IN
APPLIED MATHEMATICS, IN THE SCHOOL OF SCIENCE,
UNIVERSITY OF ELDORET, KENYA**

JUNE, 2021

DECLARATION

Declaration by the candidate

This thesis is my original work and has not been submitted for any academic award in any institution; and shall not be reproduced in part or full, or in any format without prior written permission from the author and/or University of Eldoret

Signature: Date:.....

CHIRCHIR CHERUIYOT AMOS

SSCI/MAT/M/002/18

Declaration by the Supervisors

This thesis has been submitted with our approval as University supervisors.

Signature:.....Date:.....

DR. KANDIE K. JOSEPH

Department of mathematics and computer science

University of ELdoret, Kenya

Signature:.....Date:.....

DR. JULIUS S. MAREMWA

Department of mathematics and computer science

University of Eldoret, Kenya

DEDICATION

This thesis is dedicated to my wonderful wife Gladys, my two boys Ryan and Bravin, and my friends.

ABSTRACT

In this study, we examined the flow from two lateral inflow channels in a man-made open rectangular channel of an incompressible Newtonian fluid. The influence of cross-sectional area, length of two lateral inflow channels, and angles as they vary directly proportionally to each other for two lateral inflow channels from zero to ninety degrees on how they affect the flow rate in the main rectangular open channel were investigated. When the flow rate increases, the discharge increases as well, and when the flow velocity decreases, the discharge decreases as well, since the discharge is directly proportional to the flow velocity. The flow-regulating equations are the continuity and momentum equations of motion that are extremely nonlinear and cannot be solved by an exact method. The method of finite differences is then used to numerically compute an approximate solution to these partial differential equations because of its precision, consistency, stability and convergence. MATLAB software used to generate the results which are analyzed using graphs. The analysis found that the rise in lateral inflow channels' cross-sectional area increase the flow velocity in the main channel and decrease in lateral inflow channel length increases the flow velocity in the main channel. Furthermore, inclined lateral inflow channels at 45° increase the main channel's flow velocity more than 60° and 72° , while 90° maintains the main channel's flow velocity constant.

TABLE OF CONTENTS

DECLARATION.....	ii
ABSTRACT.....	iv
LIST OF FIGURES.....	vii
LIST OF TABLES.....	viii
LIST OF NOTATIONS.....	ix
ACKNOWLEDGEMENT.....	xi
CHAPTER ONE.....	1
INTRODUCTION.....	1
1.1 Background Information.....	1
1.2 Definitions of basic concepts.....	4
1.2.1 Fluid.....	4
1.2.2 One dimensional flow.....	4
1.2.3 Unsteady flow.....	4
1.2.4 Incompressible flow.....	5
1.2.5 Viscosity.....	5
1.2.6 Inertia forces.....	6
1.2.7 Froude number.....	6
1.2.8 State of flow.....	6
1.2.9 Reynolds number, Re.....	7
1.2.10 Type of open channel.....	7
1.2.11 Saint Venant equation.....	8
1.3 Statement of the problem.....	9
1.4 Objectives of study.....	10
1.4.1 General objective.....	10
1.4.2 Specific objectives.....	10
1.5 Justification.....	10

CHAPTER TWO	12
LITERATURE REVIEW	12
METHODOLOGY	17
3.1 Mathematical model case.....	17
3.2 Mathematical formulation.....	18
3.2.1 Continuity equation (conservation of mass)	18
3.2.2 Momentum equation	20
3.2.3 Solution procedure	21
CHAPTER FOUR.....	24
RESULTS AND DISCUSSION	24
4.1 Results.....	24
4.2 Discussion	26
CONCLUSION AND RECOMMENDATION	29
5.1 Conclusion	29
5.2 Recommendation	29
REFERENCES.....	30
APPENDICES	34
APPENDIX I: MATLAB codes of effect of area on velocity	34
APPENDIX II: MATLAB codes of effect of lateral inflow length on velocity	38
APPENDIX III: MATLAB codes of effect of angle on velocity	42
Appendix IV: Similarity Report.....	46

LIST OF FIGURES

Figure 1: Mathematical model case	17
Figure 2: Effect of area on velocity	24
Figure 3: Effect of length on velocity	25
Figure 4: Effect of angle on velocity	26

LIST OF TABLES

Table 1: Velocity versus time: Area =0.01,100,400,800	37
Table 2: Velocity versus time: L=10,100,1000,10000	41
Table 3: Velocity versus time: Angle = $\pi/4$, $\pi/3$, $\pi/2.5$, $\pi/2$	45

LIST OF NOTATIONS

v	Mean velocity of flow (m/s)
L	Length of the lateral inflow channel (m)
g	Acceleration due to gravity (ms^{-2})
Q	Discharge in the main channel (m^3s^{-1})
Q_1 and Q_2	Discharge of the lateral inflow channels (m^3s^{-1})
A	Flow's cross-sectional area (m^2)
n	The roughness manning coefficient ($\text{Sm}^{-1/3}$)
S_o	The channel's bottom slope
S_f	Friction slope $= \frac{n^2 v^2}{R^{\frac{4}{3}}}$
T	Top width of free surface (m)
y	Depth of flow (m)
y_1 and y_2	is the depth on the two lateral inflow respectively (m)
t	Time (s)
q	Lateral uniform inflow (m^3s^{-1})
R	Hydraulic radius (m)
x	Distance along the main flow direction (m)
θ_1 and θ_2	Angle of lateral discharge channel in degrees

Δ	forward difference
$\frac{\partial A}{\partial t}$	Rate of change in area of flow with time (m ² /s)
$\frac{\partial v}{\partial x}$	The rate at which the flow's mean velocity changes with distance (m/s)
$\frac{\partial y}{\partial x}$	Rate of change of depth of flow with distance (m/s ²)
$\frac{\partial Q}{\partial x}$	Rate of change in discharge with distance (m ² /s)
T ₃	Top width of the main channel (m)
T ₁ &T ₂	Top width of the two lateral inflow channels (m)
c	Resistance coefficient of flow (Chezy coefficient)

ACKNOWLEDGEMENT

I wish to extend my appreciation to University of Eldoret family as a whole and to my supervisors; Dr. Kandie K. Joseph and Dr. Julius S. Maremwa for their continued guidance in preparing this thesis. My sincere gratitude also goes to my course mates and friends for their technical, moral encouragement and continuous support during the entire process.

CHAPTER ONE

INTRODUCTION

1.1 Background Information

In 2018, 2019 and 2020, Kenya experienced heavy rainfall, resulting in bridges being swept away as rivers flooded and dams shattered their walls. Examples of this environmental disaster that occurred in 2018 are the Solai Dam in Nakuru, Kenya, which breached its walls and killed 47 people after it broke its walls and swept all important resources like houses, trees, vehicles, animals and people in that village. More so, in 2019 West Pokot land slide took place and roads were blocked and some bridges were swept away. In addition, Nakuru, Elgeyo Marakwet, Baringo, Nandi, Kisumu and many others are still affected by floods during normal rainfall. As of June 30th, 2020 the Kenya Red Cross Society reported in the Floods Situational Report that due to the experienced enhanced rainfall (MAM 2020) over most parts of the country resulting in landslides, flooding of rivers and displacement of people as more homes and household assets got destroyed. A total of 43 counties out of 47 counties reported floods effects with the most displacement in West Kenya region, Coastal region, North Eastern and North Rift region. The total number of displaced Households by floods was recorded as 42,064 HH affecting over 252,384 persons by end of June 2020. It is therefore very important to design channels that regulate such an environmental catastrophe and, more importantly, use the same water to irrigate agricultural land. The fact that the flood problem still persists and the need to transport water for irrigation is still in demand means that an efficient channel model with two lateral inflows is needed to convey the maximum discharge.

Open channels are known to be channels with an open top, while channels with a closed top are called closed channels. Good examples of open channels are rivers and streams while examples of closed conduits are pipes and tunnels. Open channels made of earth and concrete have been designed which have been of different cross-sections such as trapezoidal, rectangular and circular.

In the world at large, engineers have attempted, among other things, to channel water to a specific location, Irrigation grids and dams for power generation are examples. In Kenya, most road networks lack efficient drainage systems, especially rural roads; hence, road carnage, fatalities, and economic devastation are all too common, particularly when it rains. This has a negative effect on the achievement of Kenya's 2030 vision that aims to create a high-quality, internationally competitive and prosperous nation by 2030. There are three main pillars of the 2030 vision that the government aims to accomplish. These are foundations of economic, political and social value. These three pillars are connected to our research due to the fact that inadequate drainage directly affects people's economy. For example, transport is disrupted when it rains and roads are cut off by runoff, and this affects the flow of goods and services. Large amounts of cash are often used to repair bridges, sewers, airports and playgrounds. Due to the blockade of sewers and highways, people have also gone on strike and this affects the smooth running of businesses. In addition, Diseases outbreaks and other related health issues pose a danger to the population's health if drainage is insufficient. As a result, our study aims to find solutions to these drainage-related issues in order to contribute to the 2030 vision.

Following researches which has been done by different researchers for example Jomba et al (2015) investigated fluid flow in an open channel with a horseshoe cross-section, Ojiambo et al (2014) and Tsombe et al (2011) did an investigation that focused on

unsteady non-uniform flow on open channels with circular cross-section, Tuitoek and Hicks (2001) investigated flood management by simulating compound channels with erratic flow in order to better manage floods. By developing a model based on the Saint Venant equations of flow, they added some terminology in order to account for the momentum phenomenon of move to integrate an inconsistency in the flow in the compound channels and for open channel flows with uniform and localized lateral inflow, Fan and Li (2005) developed diffusive wave equations. In their formulation, they provided the continuity and momentum equations for an open channel with a lateral inflow channel intersecting the main open channel at a differing angle, Mohammed (2013) studied how four different angles affect the discharge coefficient by using an oblique weir in the flow direction, in comparison to the side of the channel floor. 30° , 60° , 75° , and 90° were the four angles that changed depending on the direction of flow and more so Karimi et al. (2014) and Samuel M.K. (2020) conducted research on fluid modeling in the case of a single inflow channel on an open rectangular channel and open trapezoidal channel respectively.

According to the literature, a lot of research appears to have been done in open channels with no two lateral inflow channels. The research on the lateral inflow channel, on the other hand, has only been done in a single inflow channel and laboratory. As a result, little research has been done in open channels with two lateral inflow channels using mathematical modeling and numerical solutions.

As a result, the problem is mathematically modeled using the Saint Venant equations, and the equations are solved using the finite difference method in this study.

The analysis would focus on appropriate cross sectional area, lateral inflow length and angles to align with two inflow channels in order to aid in the prevention of drainage

channel blockages, which are a frequent occurrence in drainage systems. We hope that the results of this study will be useful in the design of drainage systems for road construction, sewer building, street drainage, long dams, and airport construction in Kenya and elsewhere.

1.2 Definitions of basic concepts

Several terms will be used extensively in this thesis, and these terms are described in this section.

1.2.1 Fluid

Fluid is a matter which has been classified as liquids and gases. According to Brownian motion and kinetic theory of matter, it is made up of tiny particles. If pressure and temperature are applied to liquid and the volume changes are negligible then we treat as incompressible fluids while gases change dramatically and volume change is significant hence it is compressible.

1.2.2 One dimensional flow

This is the case of a fluid in which all fluid particle flows move in one direction.

Mathematically, it is written as

$$u=f(x) \quad (\text{in } x \text{ direction})$$

Where u and x is the velocity and space coordinate.

1.2.3 Unsteady flow

Unsteadyflow refers to flow in which the velocity, pressure, or density varies with regard to a certain point in time.

Mathematically, it is written as

$$\left(\frac{\partial v}{\partial t}\right) \neq 0$$

$$\left(\frac{\partial p}{\partial t}\right) \neq 0$$

$$\left(\frac{\partial \rho}{\partial t}\right) \neq 0$$

1.2.4 Incompressible flow

This refers to type of flow in which the density is constant, or its change is negligible, or no change at all.

Mathematically, written as: $\rho = \text{constant}$

1.2.5 Viscosity

The resistance to flow is referred to as viscosity. Fluidity is the reciprocal of viscosity which is a measure of how quickly something moves. Molasses has a higher viscosity than oils, for example. Viscosity can be thought of as internal friction between the molecules, as part of a fluid that is required to flow carries over neighboring parts to some degree; such friction is opposed to the creation of variations in velocity within a fluid. The shear pressure divided by the rate of shear strain for a given fluid at a fixed temperature is constant. The viscosity dynamic, or absolute, or merely the viscosity are two terms for the same constant.

Fluids that behave in this manner are referred to as Newtonian fluids after Sir Isaac Newton, who first suggested this scientific concept of viscosity.

The dynamic viscosity dimensions = $\frac{\text{Force} \times \text{Time}}{\text{Area}}$

The unit of viscosity is Newton-second per square meter, commonly expressed in SI units as Pascal-second.

1.2.6 Inertia forces

These are forces that cause the acceleration of the fluid particles in motion to be zero. They resist change in the velocity of an object and are in the opposite direction of an applied force.

1.2.7 Froude number

The dimensionless Froude number is important in analyzing the effect of gravity in fluid flow. It's the ratio of inertial forces to gravitational forces. Mathematically is written as:

$$Fr = \frac{V}{\sqrt{gD}},$$

Where the hydraulic depth is D , the mean velocity is V and the gravity acceleration is g . If Fr is one, it means that the inertial forces and gravity force are equivalent and critical flow exists.

1.2.8 State of flow

The viscosity effects control the state of open channel flow in relation to the inertial forces of the flow. Depending on the influence of viscosity relative to the forces of inertia, the flow may be laminar, transitional or turbulent. The fluid particles tend to travel in thin layers of fluid in laminar flow that appear to slip over neighboring layers with no interruptions between the layers. If the inertial forces are strong compared to the viscous forces, the flow is turbulent. The fluid particles travel in irregular directions during turbulent flow. When it is neither laminar nor turbulent, a flow is called transitional.

1.2.9 Reynolds number, Re

This is a number without dimensions and is the proportion of forces of inertia to viscous forces.

Mathematically is written as:

$$Re = \frac{\rho VL}{\mu} = \frac{VL}{\nu}$$

The kinematic viscosity is ν , the mean flow velocity is V , and the characteristic length is L . Depending on the Reynolds number, the flow in the channel alters from laminar to turbulent. The flow is laminar if Re is less than approximately 2000 and the flow is turbulent if Re is greater than 4000. If it is between these values, the flow is in transition. It is understood that laminar flow occurs where thin sheets of water flow or where conditions are modified, as in model testing.

1.2.10 Type of open channel

There are two kinds of channels that are available, namely natural and artificial ones. Artificial channels are manmade channels. They include irrigation canals, canals for navigation, spillways, sewers, culverts, and ditches for drainage. They're usually designed with a clear cross-section shape all the way around. They are usually built of concrete in the field and have relatively well defined surface roughness, although this can change with age. The flow in such channels would yield relatively accurate results when analyzed.

Natural channels are not common and their materials can vary widely. The roughness of the surface varies with time, distance, and elevation. As a result, studying natural channels correctly and achieving acceptable results is more difficult than analyzing man-made channels. If the boundary is not set due to erosion and sediment deposition,

this condition can be more complicated. Various geometric properties of the channel cross-sections are required for study. This can normally be described for artificial channels using simple geometric equations given the flow depth.

1.2.11 Saint Venant equation

It was developed by two Mathematicians, De Saint Venant and Bousinnesque, in the nineteenth century from Navier equation for shallow water flow condition and one dimension. Dynamic routing is the solution to the St. Venant equation, and it is often used to measure or compare other techniques. In open channels, it is the equations that characterize the propagation of a flood wave in terms of distance along the channel and time. It is made up of two equations: the continuity equation and the momentum equation. The inertial terms appearing in the momentum equation of the Saint-Venant equation can be ignored for most flood events in most rivers because they are comparatively smaller than the terms arising from gravity and resistance forces Henderson(1963), resulting in a simplified model of open channel flow. The shallow water wave propagation in open channels is represented by the Saint–Venant hydrodynamic equations, which are obtained from the depth-averaged Navier–Stokes equations. For a rectangular channel, the one-dimensional Saint–Venant equations are as follows (Chow 1959):

Continuity equation (Conservation form).....(1.1)

$$\frac{\partial Q}{\partial x} + \frac{\partial A}{\partial t} = 0$$

Momentum Equation.....(1.2)

$$\frac{1}{A} \frac{\partial Q}{\partial t} + \frac{1}{A} \frac{\partial}{\partial x} \left(\frac{Q^2}{A} \right) + g \frac{\partial y}{\partial x} - g(S_o - S_f) = 0$$

From equation (1.1) and (1.2) Q is the discharge, A cross sectional area, g gravitational force, y is the depth, s_0 bottom slope and s_f frictional slope

Saint Venant suggested the above governing equations for one-dimensional unsteady flow in an open channel in 1871, which included continuity and momentum equations, and Shang et al (2012) research on the equation and confirm that it is a true equation to analyses one dimensional unsteady flow in an open channel.

The Saint-Venant equations, also known as the dynamic wave model, are the governing equations for conservation of mass and momentum for unsteady open channel flow Chanson (2004). Solving these equations requires large amounts of data to prescribe channel geometry along the reach and elaborate numerical integration to ensure accuracy and convergence Szymkiewicz (2010) and more so simplified forms of the equations have been sought over the years that may be easier to use in practical applications such as operational flood forecasting. Among the most frequently used simplifications is the diffusive wave approximation which neglects the inertial terms. Though a more appropriate name “noninertia wave” has been proposed Yen and Tsai (2001), the term diffusive wave is still widely used which is also adopted here to avoid confusion. The diffusive wave model is attractive for a number of reasons Cappelaere (1997). It combines the system of equations into a single equation of a single state variable of flow.

1.3 Statement of the problem

Extensive fluid flow studies have been performed across open channels.

Open channel Mathematical modeling with two lateral inflow channels has received little attention, however. The aim of this study is to see how the area, length, and angle

of the two lateral inflow channels influence the rate of flow of the open rectangular channel as it varies. The fluid in question is Newtonian, and the flow is slow. Therefore, this research is intended to establish an adequate flow model through two lateral inflow channels in a rectangular open channel.

1.4 Objectives of study

1.4.1 General objective

Analyze the flow of fluid in an open rectangular channel on the main flow with two lateral inflow channels in order to find suitable cross sectional area, lateral length and angle.

1.4.2 Specific objectives

1. To investigate the effect of variation in the cross-sectional area of two lateral inflow channels on velocity in the main open channel.
2. To investigate the effect of variation in the length of the two lateral inflow channels on velocity in the main open channel.
3. To investigate the effect of variation in the angles of the two lateral inflow channels on velocity in the main open channel.

1.5 Justification

To live and grow every living thing it needs water but excess of it will lead to death. In order for water to be regulated smoothly by lakes and rivers, men must create adequate channels. In Kenya the flood problem still exists, particularly when there is heavy rain or poor drainage, e.g. Narok town and some flat sections. Creating a channel that has two lateral inflow channels that it can effectively transmit the maximum amount of water remains a challenge so far. Therefore, an effective open channel model with two lateral channels of inflow must be built to meet these requirements. This study's

mathematical model can be used to make two lateral inflow channels to improve discharge while carrying transporting water to farms for irrigation and water drainage from flood-stricken areas. Furthermore, the model can be used in industries such as flour or garment manufacturing, as well as in the installation of water mills, which involve vast amounts of high-speed water to transform large turbines to power mechanical processes.

CHAPTER TWO

LITERATURE REVIEW

The literature review in this chapter deals with review of the equation that govern open channel flow, lateral inflow studies and numerical methods used and finally the summary why there is a gap in the literature to conduct the present study.

Jomba et al (2015) investigated fluid flow in an open channel with a horseshoe cross-section. From the study he established that for a fixed flow area, the flow velocity increases as depth increases towards the free stream. Also he established that an increase in hydraulic radius and roughness coefficient results to a reduction of velocity due to increased shear stresses. Tuitoek and Hicks (2001) investigated flood management by simulating compound channels with erratic flow in order to better manage floods. By developing a model based on the Saint Venant equations of flow, they added some terminology in order to account for the momentum phenomenon of move to integrate an inconsistency in the flow in the compound channels.

Ojiambo et al (2014) did an investigation that focused on unsteady non-uniform flow on open channels with circular cross-section. The findings were that an increase in the cross-sectional area and depth of flow leads to decrease in the flow velocity. An increase in the lateral inflow rate per unit length of the channel leads to a decrease in the flow velocity.

Kwanza et al. (2007) studied the effects of lateral discharge and channel slope, width, velocity, and depth as they vary from one point in the channel to the next on fluid velocity and channel discharge in both trapezoidal and rectangular channels. They noted that in order to increase channel discharge, the channel's slope, width, and lateral

discharge all need to be increased. Furthermore, by reducing the wetted perimeter, the fluid flow rate increased.

Tsombe et al (2011) investigated flow in open channels having circular cross-sectional area. He found out that when the flow depth increases, it results to reduced fluid velocity. Also reduction in slope leads to a decrease in flow velocity.

Fluid flow in open rectangular and triangular channels was studied by Thiong'o (2011). Her observations on rectangular channels were close to those of Kwanza et al (2007). In an open rectangular channel, the flow velocity increased as the slope, discharge, and width increased, according to their findings. Increases in the wetted periphery of the channel, on the other side, resulted in a decrease in flow velocity. They both used the finite difference method as a computational instrument to solve the continuity and momentum equations.

The main channel's ratio of downstream to upstream discharge, as defined by Ramamurthy and Satish (1988), Ingle and Mahankal (1990), is the most important parameter in evaluating open flow with a 90° lateral channel. When these results were compared to some experimental findings, it was discovered that the study yielded satisfactory results.

The flow structure is defined by the roughness of the bed, as well as the velocity ratio between the branch and main channels, according to Neary and Odgaard (1993).

Barkdoll et al (1999) discovered that the diversion flow ratio has the greatest impact on the lateral intake sediment diffusion ratio, and is done in a straight line with a 90° intake angle.

Yang et al (2009) looked at flow systems of 90° , 45° , and 30° diversion angles. To boost the flow pattern of the fluid, a diversion angle of 30° to 45° was suggested.

For open channel flows with uniform and localized lateral inflow, Fan and Li (2005) developed diffusive wave equations. In their formulation, they provided the continuity and momentum equations for an open channel with a lateral inflow channel intersecting the main open channel at a differing angle.

When focusing on the sub-critical flow regime, Ramamurthy and Satish (1988) theoretically and experimentally investigated dividing flows with a submerged lateral branch. The researchers theoretically developed a model by relating discharge ratios and downstream-to-upstream depth to the upstream Froude number. Their findings revealed that the re-circulatory zone downstream of the junction causes a contraction in the channel section, causing the flow to change to supercritical flow. The discharge in the branch of the lateral channel can be calculated using Mizumura et al (2003)'s formula for super-critical overflowing rivers, which compared well with Mizumura (2005)'s results.

Mohammed (2013) studied how four different angles affect the discharge coefficient by using an oblique weir in the flow direction, in comparison to the side of the channel floor. 30° , 60° , 75° , and 90° were the four angles that changed depending on the direction of flow. The research discovered that the highest discharge was reached when the side weir was tilted at 30 degrees.

Masjedi and Taedi (2011) looked into the effects of intake angle on lateral intake discharge ratio with 180° bend in the laboratory. The tests were carried out with a range of Froude numbers and intake angles. At a 45° lateral intake angle, the discharge ratio improved in all locations of the 180° flume bend, according to the study.

Shamaa (2002) solved open channel operation-type problems using the finite difference Preissmann implicit construct, built on the Saint Venant equations. The implicit finite difference method model showed less oscillation and more precision as compared to an explicit model.

The diffusive schemes of Preissmann and Lax, which are two separate numerical methods for Saint Venant equations numerical solution, were investigated by Akbari and Firoozi (2010). With the aim of better understanding the propagation process, these equations regulate the flood waves propagate in natural waterways. The results of the study indicated that hydraulic parameters play a significant role in these waves.

Chagas and Souza (2005) used the study of floods in rivers to solve the Saint Venant equation. The aim of this analysis was to achieve a better understanding of the propagation process by using a discretization for the Saint Venant equations. According to their observations, hydraulic parameters play a significant part in the transmission of flood waves.

Karimi et al. (2014) conducted research on fluid modeling in the case of a single inflow channel on an open channel, and discovered that the velocity of the main open channel does not necessarily increase as the angle of the lateral inflow channel is increased. Angles between 30 and 50 degrees produce higher velocity values in the main open channel than other angles.

Omari et al (2018) did an investigation on closed channel with circular cross-sectional area. The results obtained showed that an increase in the cross sectional area of sewer flow results to a decrease in the sewer depth. It was observed that a decrease in the friction slope leads to an increase in the sewer flow velocity. Also it was found out that an increase in tunnel angle of inclination results to an increase in sewer velocity.

In a statistical model of fluid flow in an open trapezoidal channel with lateral inflow channel, Samuel M.K. (2020) found that decreasing the cross-sectional area increases flow velocity while increasing the length of the lateral inflow channel decreases flow velocity. It's also worth noting that increasing the lateral inflow channel's velocity increases the flow velocity, and that an angle of thirty to fifty degrees increased the flow velocity relative to other lateral inflow channel angles.

CHAPTER THREE

METHODOLOGY

We will review Saint Venant equations which govern open channel flow then modified to incorporate an open channel with two lateral discharges at an angle. To modify the equations then we need to adopt some assumptions

3.1 Mathematical model case

A Mathematical model of an open rectangular channel with two angled lateral inflow channels. Let Q , q_1 and q_2 be the discharge into the rectangular open channel, as well as the two lateral inflow channels, respectively. L_1 , L_2 , Θ_1 and Θ_2 reflect the length and differing angles of the two lateral inflow channels, respectively. The top width of the two lateral inflow channels and the primary channel are T_1 , T_2 and T_3 . At a time interval dt , the net amount of fluid that reaches the cell dx is taken into consideration.

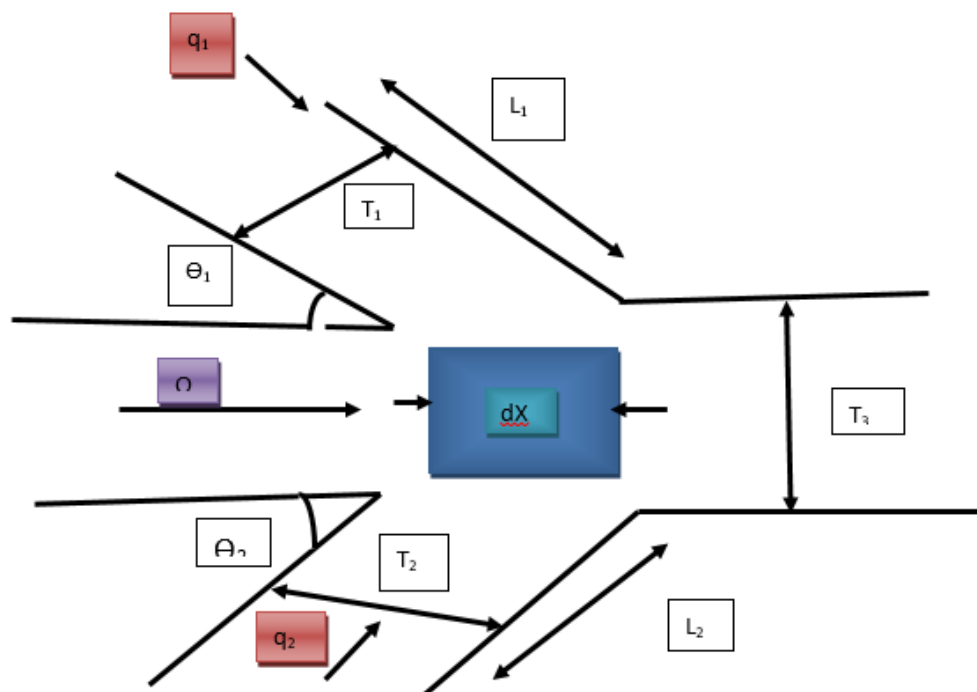


Figure 1: Mathematical model case

Assumptions to be adopted:

- i. The fluid is Newtonian
- ii. The fluid is considered incompressible where density is constant everywhere. $\rho = \text{constant}$
- iii. unsteady flow (Changes in fluid variables relative to time at a point)
- iv. Gravity alone is responsible for the forces causing the flow, and other forces produced in the junction region are ignored.
- v. The flow is one-dimensional, with the majority of momentum happening around the x-axis and being completely dependent on x.
- vi. The length, top width, depth and angles of the two inflow channels should be directly proportional to each other has follows.
 $L_1=L_2, T_1=T_2, y_1=y_2, \Theta_1=\Theta_2$
- vii. There is no substantial accumulation of small particles between the primary open channel and the two lateral inflow channels.
- viii. There is no major turbulent development between the primary open channel and the two lateral inflow channels.

We consider approximation solutions by using the finite difference method and, more importantly, the use of MATLAB tools to derive the results in diagrams, using the conditions above and combining with the continuity equation and momentum equation of motion, which will yield nonlinear equation.

3.2 Mathematical formulation

3.2.1 Continuity equation (conservation of mass)

The continuity equation is a type of differential equation that describes the movement of a conserved quantity, such as mass.

Continuity equation governing flow in an open channel that isn't consistent of any shape is provided by,

$$\frac{\partial Q}{\partial x} + \frac{\partial A}{\partial t} = q \dots\dots\dots (3.1)$$

From the model above the cell with lateral inflow dx , in a dt -interval, is considered

Total volume is $\frac{\partial Q}{\partial x} dxdt$.

Discharge from the two lateral inflow channels will be twice $\frac{q}{L} \sin \theta dxdt$ because it

has been inclined at an angle θ while increment of fluid is $\frac{\partial A}{\partial t} dxdt$ and density is

constant. Using conservation law of fluid, According to Macharia et al (2014)

we have

$$\frac{\partial Q}{\partial x} dxdt + \frac{\partial A}{\partial t} dxdt = \frac{q_1}{L_1} \sin \theta_1 dxdt + \frac{q_2}{L_2} \sin \theta_2 dxdt \dots\dots\dots (3.2)$$

Since the assumptions shown above.

$$\text{Where } q_1 = q_2 = q \quad q_1 + q_2 = 2q \quad L_1 = L_2 = L \quad \theta_1 = \theta_2 = \theta$$

Applying on equation (3.2). We get

$$\frac{\partial Q}{\partial x} dxdt + \frac{\partial A}{\partial t} dxdt = 2 \frac{q}{L} \sin \theta dxdt \dots\dots\dots (3.3)$$

It can be reduce to equation (3.4) by both sides by $dxdt$

$$\frac{\partial Q}{\partial x} + \frac{\partial A}{\partial t} = 2 \frac{q}{L} \sin \theta \dots\dots\dots (3.4)$$

A conserved quantity can neither decrease nor increase; it can only shift from one location to another. The equation, by Tsombe et al (2011), is

$$T \frac{\partial y}{\partial t} + vT \frac{\partial y}{\partial x} + A \frac{\partial v}{\partial x} - q = 0 \dots\dots\dots (3.5)$$

Substituting equation (3.4) into equation (3.5) where $q = 2 \frac{q}{L} \sin \theta$ and arranging we get

$$\frac{\partial y}{\partial t} + v \frac{\partial y}{\partial x} + \frac{A}{T} \frac{\partial v}{\partial x} = 2 \frac{q}{TL} \sin \theta \dots\dots\dots (3.6)$$

Equation (3.6) is the general equation of continuity for open channel flow with two lateral inflow channels at an angle.

3.2.2 Momentum equation

The momentum equation is used to describe the motion of fluid particles. This equation is derived from Newton's second law of motion, along with the statement that fluid stress is the sum of the viscous diffusing term plus a pressure term. This is the pace at which the system's linear momentum changes over time. From the model above in a dt-interval, the total momentum for the cell dx is $\frac{\partial QV}{\partial x} dxdt$. The lateral inflow component of velocity in the flow direction is $u \cos \theta$. Thus, lateral inflow momentum into cell dx at a time interval dt becomes $\frac{q}{L} \sin \theta u \cos \theta dxdt$.

The fluid pressure and fluid weight in the direction of flow are $g \frac{\partial(yA)}{\partial x} dxdt$ and $gA(S_f - S_o) dxdt$ respectively. The momentum increment for the dx cell is $\frac{\partial Q}{\partial t} dxdt$. Accordingly,

In the momentum equation we have, according to the conservation law, where

$$\begin{aligned} \frac{\partial Q}{\partial t} dxdt + \frac{\partial QV}{\partial x} dxdt + g \frac{\partial(yA)}{\partial x} dxdt + gA(S_f - S_o) dxdt \\ = 2 \frac{q}{L} \sin \theta u \cos \theta dxdt \end{aligned}$$

(3.7)

Noting that $Q = Av$

Substituting $Q=Av$, differentiating partially with respect to x and rearranging the equation, we get

$$\frac{\partial V}{\partial t} + v \frac{\partial V}{\partial x} + g \frac{\partial y}{\partial x} + g(S_f - S_o) = 2 \frac{q}{AL} \sin \theta (u \cos \theta - v) \dots \dots \dots (3.8)$$

Equation (3.8) is the general momentum equation of an open channel with two lateral inflow channels at varying angles.

3.2.3 Solution procedure

Since the governing equations (3.6) and (3.8) are nonlinear and thus cannot be solved exact method. Specifically, using the finite difference approach to diffusive scheme specifically forward difference to approximate the results.

We take

$$\frac{\partial v}{\partial t} = \frac{v(i,j+1)-v(i,j)}{\Delta t} \dots \dots \dots (3.9)$$

$$\frac{\partial y}{\partial t} = \frac{y(i,j+1)-y(i,j)}{\Delta t} \dots \dots \dots (3.10)$$

$$\frac{\partial v}{\partial x} = \frac{v(i+1,j)-v(i-1,j)}{2\Delta x} \dots \dots \dots (3.11)$$

$$\frac{\partial y}{\partial x} = \frac{y(i+1,j)-y(i-1,j)}{2\Delta x} \dots \dots \dots (3.12)$$

Substituting the equations (3.9), (3.10), (3.11) and (3.12) into equation (3.6)

$$\frac{y(i,j+1)-y(i,j)}{\Delta t} + v(i,j) \left(\frac{y(i+1,j)-y(i-1,j)}{2\Delta x} \right) + \frac{A}{T} \left(\frac{v(i+1,j)-v(i-1,j)}{2\Delta x} \right) = \frac{2q}{TL} \sin \theta \dots$$

.....(3.13)

Rearranging we get

$$y(i,j + 1) = \Delta t \left(-v(i,j) \left(\frac{y(i+1,j)-y(i-1,j)}{2\Delta x} \right) - \frac{A}{T} \left(\frac{v(i+1,j)-v(i-1,j)}{2\Delta x} \right) + \frac{2q}{TL} \sin \theta \right) + y(i,j) \dots \dots \dots (3.14)$$

Also substitute equations (3.9),(3.10),(3.11) and (3.12) into equation (3.8)

We get

$$\frac{v(i,j+1)-v(i,j)}{\Delta t} + v(i,j) \left(\frac{v(i+1,j)-v(i-1,j)}{2\Delta x} \right) + g \left(\frac{y(i+1,j)-y(i-1,j)}{2\Delta x} \right) + g(S_f - S_o) = \frac{2q}{TL} \sin \theta (u \cos \theta - v(i,j)) \dots \dots \dots 3.15)$$

Rearranging we get

$$v(i,j + 1) = \Delta t \left(-v(i,j) \left(\frac{v(i+1,j)-v(i-1,j)}{2\Delta x} \right) - g \left(\frac{y(i+1,j)-y(i-1,j)}{2\Delta x} \right) - g(S_f - S_o) + \frac{2q}{TL} \sin \theta (u \cos \theta - v(i,j)) \right) + v(i,j) \dots \dots \dots (3.16)$$

The velocity $u_0=10$ m/s and channel depth $y_0=0.5$ m are now used as the initial and boundary conditions in finite differences form.

Initial conditions,

$$y(0, x) = 0 \qquad v(0, x) = 0 \dots \dots \dots (3.17)$$

The boundary conditions

$$y(t, x_{initial}) = 30 \qquad v(t, x_{initial}) = 20 \dots \dots \dots (3.18)$$

$$y(t, x_{final}) = 10 \quad v(t, x_{final}) = 20 \dots\dots\dots(3.19)$$

Very small values of Δt are used to solve the two equations. We have set $\Delta x=20$ and $\Delta t=0.05$ in this analysis. It is understood that this finite difference process is convergent and numerically stable. The number of sub-divisions was taken to be 5 along the channel while it was taken to be 20 sub-divisions over the period. With reference to Kazezyilmaz-Alhan (2012) appropriate bottom slope for simulation range between 0.001 and 0.0001 and Handerson (1966) preferred a slope greater than 0.002 for simulations of the natural flood waves in rivers hence we choose 0.002.

The following constants were also considered:

$$T = 1, \quad L = 1, \quad q = 0.3, \quad \theta = \frac{\pi}{3} = 60^0, \quad g = 9.82, \quad n = 0.01,$$

$$R = 1.1$$

Lin et al (1979) used manning's formula and coefficient of $n=0.01$ throughout the study, Chung-Chieh (1998) study about flow at 90^0 equal-width open-channel junction with discharge range of $0.1 \leq Q \leq 0.9$ and he found that the results of $Q=0.1, 0.4$ and 0.8 reveal that large discharge ratios are associated with smaller depth-averaged flow angles and are less uniformly distributed across the branch channel entrance. Additionally, flow deflection at the upstream corner of the branch channel entrance increases with the discharge ratio.

The MATLAB software is used to simulate the equations (3.14) and (3.16) which appear in Appendix. This was done by varying i and j at various nodal points. Then the three graphs were plotted using the values of the velocity and the time at a certain location. Various flow parameters of area, length and angle were investigated to determine how they affect the velocity.

CHAPTER FOUR

RESULTS AND DISCUSSION

4.1 Results

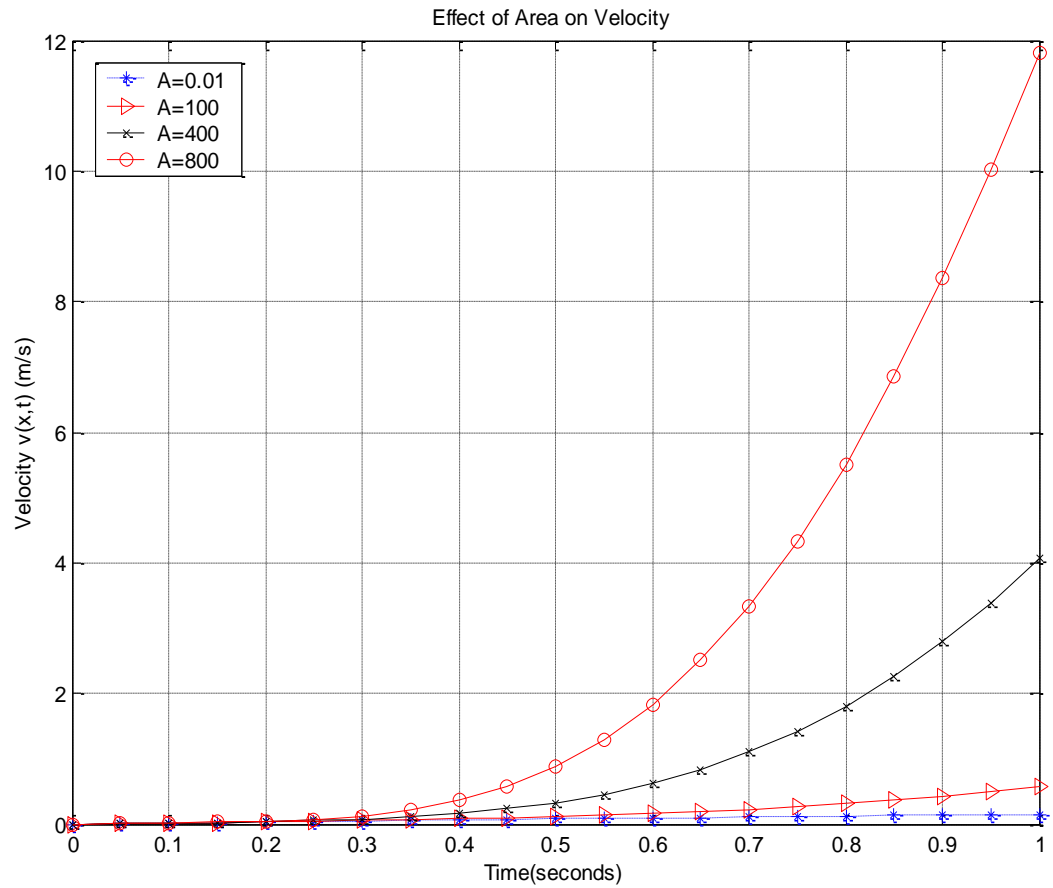


Figure 2: Effect of area on velocity

The graph above of velocity (m/s) against time (s) shows the effect of lateral cross section area in square meters.

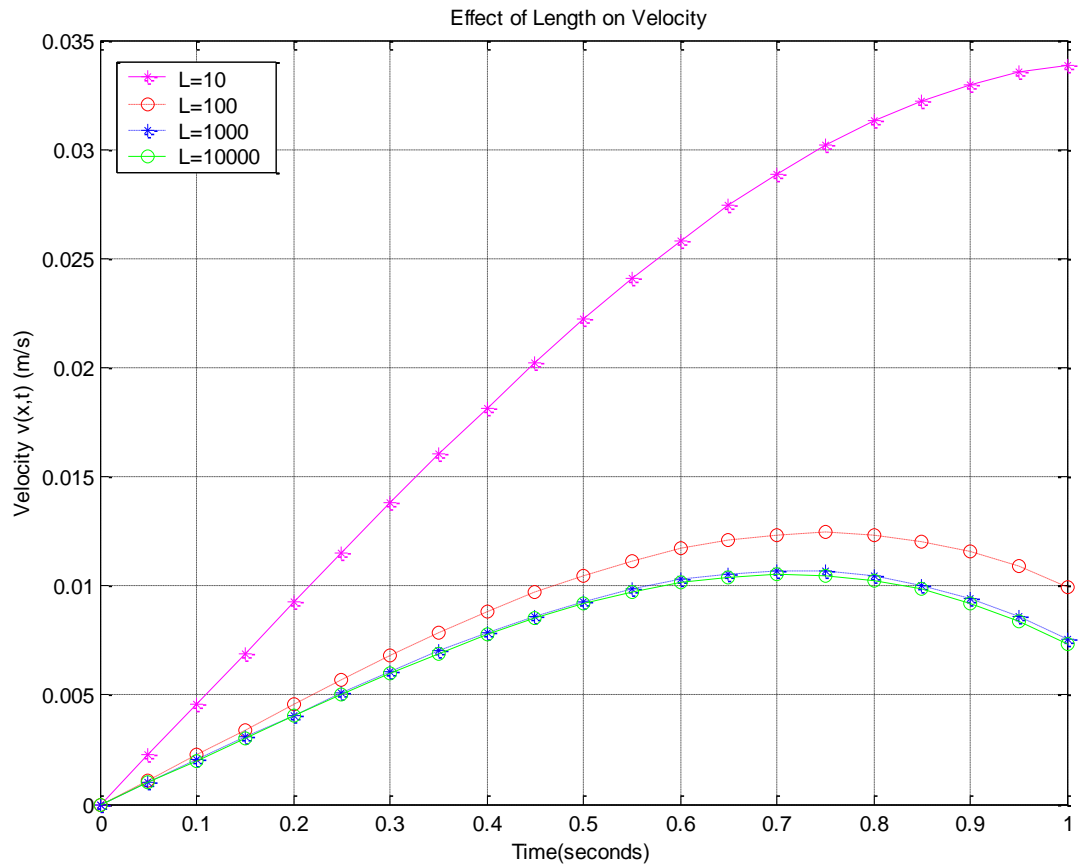


Figure 3: Effect of length on velocity

The graph above of velocity (m/s) against time (s) shows the effect of lateral length in meters.

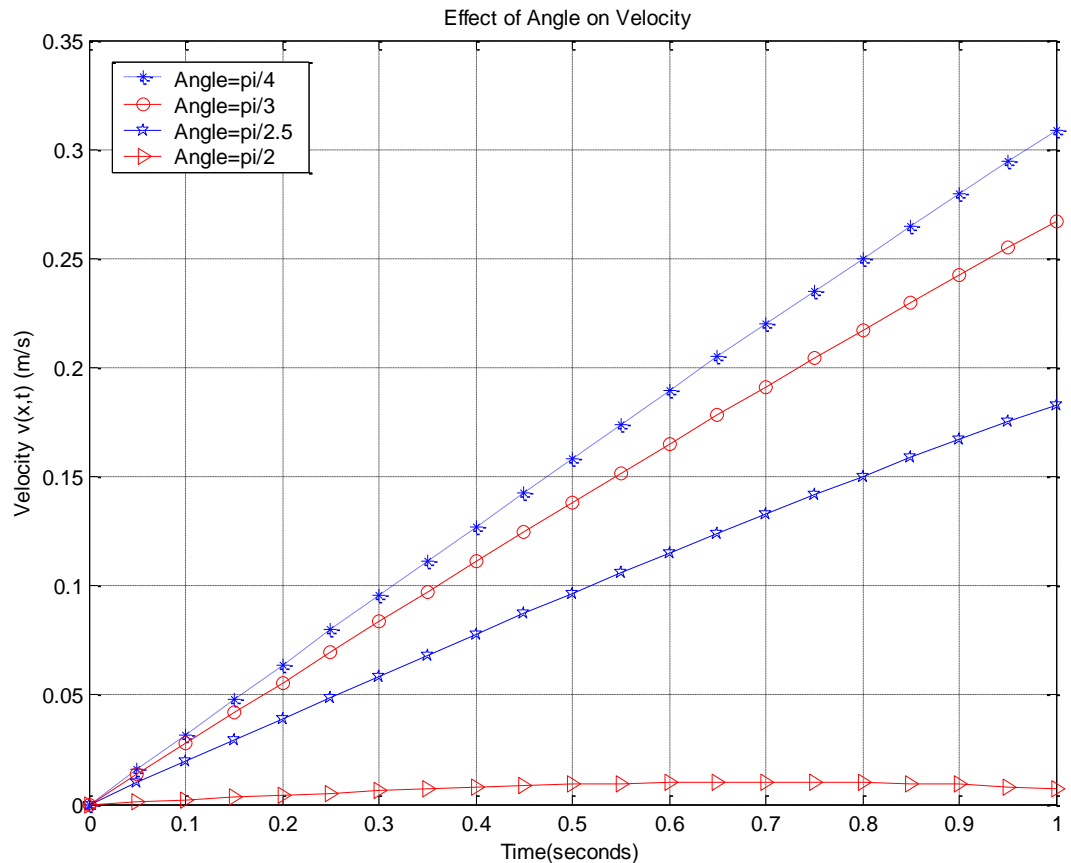


Figure 4: Effect of angle on velocity

The graph above of velocity (m/s) against time (s) shows the effect of lateral angle in degrees.

4.2 Discussion

Figure 2 indicates that the rise in the area of the two lateral inflow channels raises the discharge to the main channel in those channels and thus also increases the flow rate of the main channel as the increase in the discharge causes the velocity to increase with the constant the primary channel's cross-sectional area.

Figure 3 shows that raising the length from 10 m to 10,000 m allows the flow velocity to decrease. This is due to the fact that as the length of the fluid channel increases, the moist perimeter under the fluid channel grows as well. Wetted elevation of the

perimeter implies an increase in shear stress at the bottom of the conduit, leading to a decrease in the velocity of flow. The inflow channel length of 10m is the effective length for further discharge to occur.

Figure 4 shows that the rise in the angle above 45° contributes to a decrease in the velocity of the flow. The flow velocity is constant at 90° , indicating no impact induced by the fluid from the lateral inflow channels, and from the above assumption, we conclude that the flow is laminar, so there is no turbulence in the junction.

The inflow channel angle of 45° is the most efficient angle for further discharge.

In general, we advise designers to consider the shorter length of the lateral inflow channel (10m) and the angle of 45° for optimum discharge to occur in flat areas.

The results obtained from this study were found to be in line with what other researchers have investigated and found for instance, Kwanza et al. (2007) studied the effects of lateral discharge and channel slope, width, velocity, and depth as they vary from one point in the channel to the next on fluid velocity and channel discharge in both trapezoidal and rectangular channels. They noted that in order to increase channel discharge, the channel's slope, width, and lateral discharge all need to be increased. Furthermore, by reducing the wetted perimeter, the fluid flow rate increased.

Yang et al (2009) looked at flow systems of 90° , 45° , and 30° diversion angles. To boost the flow pattern of the fluid, a diversion angle of 30° to 45° was suggested.

Masjedi and Taedi (2011) looked into the effects of intake angle on lateral intake discharge ratio with 180° bend in the laboratory. The tests were carried out with a range

of Froude numbers and intake angles. At a 45° lateral intake angle, the discharge ratio improved in all locations of the 180° flume bend, according to the study.

CHAPTER FIVE

CONCLUSION AND RECOMMENDATION

5.1 Conclusion

The goal was to look at the impact of the area, length and angle of the lateral inflow channels on the main channel flow velocity. The following are the summary;

- i. Increasing the lateral inflow channel area increases the discharge in the inflow channels, thus increasing the main channel flow velocity.
- ii. As the lateral length of the inflow increases, the main channel flow rate decreases.
- iii. The angle of 90° does not affect the key channel's flow velocity. 72° and 60° increases but 45° increases more the flow velocity.

5.2 Recommendation

There is still a room for verification of these theoretical results with laboratory results. The geometrical model above can be developed in laboratory for more investigation.

We recommended that future research can be done on;

- i. The effect of the slope, energy coefficient, top width and other parameters of inflow channels on the main channel on the flow velocity.
- ii. The flow in trapezoidal, circular, triangular with two lateral inflow channels in different point of the main flow.

REFERENCES

- Akbari, G. and Firoozi, B. (2010). Implicit and Explicit Numerical Solution of Saint Venant Equations for Simulating Flood Wave in Natural Rivers. *5th National Congress on Civil Engineering, Ferdowsi University of Mashhad, Mashhad, Iran.*
- Barkdoll, BD, Ettema, R. and Odgaard, AJ. (1999). Sediment Control at Lateral Diversions: Limited and Enhancements to Vane Use. *Journal of Hydraulics Engineering*, 125(8):862–870.
- Cappelaere, B. (1997). Accurate diffusive wave routing. *Journal of Hydraulic Engineering*, 123(3), 174–181.
- Chagas P. and Souza R. (2005). Solution of Saint Venant’s Equation to Study Flood in Rivers, through Numerical Methods. *Paper1 Conf AGU Hydrology Days.*
- Chanson, H. (2004). Environmental hydraulics for open channel flows. Burlington, MA: *Elsevier.*
- Chow, V. T. (1959). Open-Channel Hydraulics. *New York: McGraw Hill Book Company*, 1-40.
- Chung-Chieh Hsu,t Associate Member, ASCE, Feng-Shuai Wu/ and Wen-Jung Lee (1998). “flow at 900 equal- width open- channel junction” *J. Hydraul. Eng.* 1998.124:186-191
- Fan, P. and Li, J.C. (2005). Diffusive wave solutions for open channel flows with uniform and concentrated lateral inflow. *Advances in Water Resources*, 1000–1019.

- Henderson, F. M.: Flood waves in prismatic channels, *ASCE J. Hydr. Div.*, 89, 39–67, 1963.
- Ingle, R.N. and Mahankal, A.M. (1990). Discussion of 'Division of Flow in Short Open Channel Branches.' by A.S. Ramamurthy and M.G. Satish. *Journal of Hydraulics Engineering*, 116(2), 289-291.
- Jomba J, Theuri D.M, Mwenda E, Chomba C (2015) “Modeling fluid flow in open channel with horseshoe cross-section”. *International Journal of Engineering and Applied Sciences*5.
- Kazezyılmaz-Alhan, C. M.: An improved solution for diffusion waves to overland flow, *Appl. Math. Model.*, 36, 4165–4172, 2012.
- Kwanza, J. K., Kinyanjui, M. and Nkoroi, J.M. (2007). Modeling fluid flow in rectangular and trapezoidal open channels. *Advances and Applications in FluidMechanics*, 2, 149-158.
- Lin, J. D., and Soong, H. K. (1979). "Junction losses in open channel flows," *Water Resour. Res.*, 15,414-418.
- M.T.Shamaa (2002). A Comparative Study of Two Numerical Methods for Regulating Unsteady Flow in Open Channels. Irrigation & Hydraulics Dept., *Faculty of Engineering, Mansoura University, Egypt*.
- Macharia Karimi, David Theuri and Mathew Kinyanjui. Modelling Fluid Flow in an Open Rectangular Channel with Lateral Inflow Channel. *International Journal of Sciences: Basic and Applied Research (IJSBAR)*, Vol 17, No 1 (2014), 186-193.

- Maranga PK, Mwenda E, Theuri DM (2016) modeling open channel fluid flow with trapezoidal cross section and segment base. *J Appl computat math* 5:292
- Masjedi, A. and Taeedi, A. (2011). Experimental Investigations of Effect Intake Angle on Discharge in Lateral Intakes in 180 Degree Bend. *World Applied Sciences Journal*, 15 (10), 1442-1444.
- Mizumura, K. (2005). Discharge ratio of side outflow to supercritical channel flow. *Journal Hydraulic Engineering*, 129.
- Mizumura, K., Yamasaka, M. and Adachi, J. (2003). Side outflow to supercritical channel flow. *Journal Hydraulic Engineering*, 129.
- Mohammed, A.Y. (2013). Numerical analysis of flow over side weir. *Journal of King Saud University Engineering Sciences*. Retrieved from :
<http://dx.doi.org/10.1016/j.jksues.2013.03.004>
- Neary, V.S. and Odgaard, A.J. (1993). Three-Dimensional Flow Structure at Open Channel Diversions. *J. Hydr. Engrg. ASCE.* , 119(11), 1223-1230.
- Ojiambo V.N, Kinyanjui M. N, Theuri D.M. Kiogora P.R. Giterere K (2014) “Modeling Fluid Flow in Open Channel with Circular Cross-section”, *International Journal of Engineering Science and Innovative Technology*, 3 (5).
- Omari P.I, Sigey J.K, Okelo J.A and Kiogora R.P (2018) “Modeling circular closed channels for Sewer lines”. *International Journal of Engineering Science and Innovative Technology (IJESIT)*, 7(2).
- Ramamurthy, A.S. and Satish, M.G., (1988). Division of Flow in Short Open Channel Branches. *J. Hydr. Engrg. ASCE*, 114(4), 428-438.

- Samuel M.K. (2020) “A Mathematical Model of Fluid Flow in an Open Trapezoidal Channel with Lateral Inflow Channel.” *International Journal of Sciences: Basic and Applied Research (IJSBAR)* (2020) Volume 54, No 3, pp 174-182
- Shang, Y.; Liu, R.; Li, T.; Zhang, C.; Wang, G (2011). Transient flow control for an artificial open channel based on finite difference method. *Sci. China Technol. Sci.* **2011**, *54*, 781–792. [Google Scholar] [CrossRef]
- Szymkiewicz, R. (2010). Numerical Modeling in Open Channel Hydraulics (Vol. 83). *Springer Science & Business Media*.
- Thiong’o, J.W. (2011). Investigations of fluid flows in open rectangular and triangular channels (Master’s thesis). *J.K.U.A.T, Juja, Kenya*.
- Tsombe DP, Kinyanjui MN, Kwanza JK, Giterere K (2011) Modeling fluid flow in open channel with circular cross-section. *Jagst* 13: 80-91.
- Tuitoek, D. K. and Hicks, F. E. (2001). Modelling of unsteady flow in compound channels. *African Journal of Civil Engineering*, 4, 45-53.
- Viessman W., Jr., Knapp, J.W., Lewis, G.L. and Harbaugh, T.E.(1992). Introduction to hydrology, Second edition. *Harper & Row. New York*, pp. 1-60.
- Yang, F., Chen, H. and Guo, J. (2009). Study on “Diversion Angle Effect” of Lateral Intake Flow. *33th IAHR Congress, Vancouver, Canada*, 4509-4516.
- Yen, B. C., & Tsai, C. W.S. (2001). On noninertia wave versus diffusion wave in flood routing. *Journal of Hydrology*, 244(1), 97–104. [https://doi.org/10.1016/S0022-1694\(00\)00422-4](https://doi.org/10.1016/S0022-1694(00)00422-4)

APPENDICES

APPENDIX I: MATLAB codes of effect of area on velocity

```

% Date: 24/01/2021

% Numerical Study of Fluid Flow in an open rectangular Channel

% #####

% solve  $y_t + v \cdot y_x + (A/T)v_x = (2q/TL)\sin(\theta)$   $0 \leq x \leq xf$ ,  $0 \leq t \leq t_{final}$ 

%  $v_t + v \cdot v_x + g y_x + g(sf-s_0) = (2q/AL)\sin(\theta)(\cos(\theta) - v)$   $0 \leq x \leq xf$ ,  $0 \leq t \leq t_{final}$ 

% Initial Condition:  $y(x,0) = ity_0(x)$ 

%  $v(x,0) = itv_0(x)$ 

%

% Boundary Conditions:  $y(0,t) = g_0(t) = by_0(t)$  (left BC)

%  $y(xf,t) = g_1(t) = by_1(t)$  (right BC)

%  $v(0,t) = h_0(t) = bv_0(t)$  (left BC)

%  $v(xf,t) = h_1(t) = bv_1(t)$  (right BC)

clc,clf,clear all,close all% clear screen,clear figure,clear all declared variables, close all
figures

T=1; % Top width

L=1; % Lateral length

q=0.3; % Discharge

theta=pi/3; % Angle of discharge

g=9.82; % gravitational force

s0=0.002;

n=0.01;R=1.1;

u=10;

```

```

t0=0;          % initial time

x0=0;          % initial distance

xfinal=100;    % maximum distance final distance/distance at which concentration is
to be calculated

tfinal=1;      % maximum time (final time)

M=5;           % M = # of subintervals along x(distance) axis

N=20;          % N = # of subintervals along t(time) axis

dx = (xfinal-x0)/M ; % distance interval

x = [0:M]*dx;  % values of distance (x)

dt = (tfinal-t0)/N; % time interval

t = [0:N]*dt;  % values of time (t)

% initial and boundary conditions formulae definitions(next three lines)

ity0=inline('0','x','t');itv0=inline('0','x','t');

by0=inline('30','x','t');bv0=inline('20','x','t');

byf=inline('10','x','t');bvf=inline('20','x','t');

for i = 1:M + 1,

    y(i,1) = ity0(x(i),t(1)); % initial condition evaluation

    v(i,1) = itv0(x(i),t(1)); % initial condition evaluation

end

for j = 1:N + 1

    y(1,j) = by0(x(1),t(j)); % boundary conditions evaluations

    y(M+1,j)=byf(x(M+1),t(j)); % boundary conditions evaluations

    v(1,j) = bv0(x(1),t(j)); % boundary conditions evaluations

    v(M+1,j)=bvf(x(M+1),t(j)); % boundary conditions evaluations

end

```

```

% if gt(dt/(2*dx),1)                % stability condition: 2*D_L*dt/dx^2 <= 1
%   error('stability condition not satisfied') % error message if stability condition is
not satisfied
%   return                            % return control to command line
% end                                  % end of stability condition loop

for A=[0.01 100 400 800]

for j = 1:N                            % start of time loop
    for i = 2:M                          % start of distance loop
        y(i,j+1)=dt*(-v(i,j).*((y(i+1,j)-y(i-1,j))/(2*dx))-(A/T)*((v(i+1,j)-v(i-
1,j))/(2*dx)))+(2*q/(T*L))*sin(theta))+y(i,j)
        v(i,j+1)=dt*(-v(i,j).*((v(i+1,j)-v(i-1,j))/(2*dx))-g*((y(i+1,j)-y(i-1,j))/(2*dx))-
g*(n^2*(v(i,j).^2/R^(4/3))-s0)+(2*q/(T*L))*sin(theta)*(u*cos(theta)-v(i,j))))+v(i,j)
    end                                  % end of distance loop
end                                      % end of time loop

plot(t,v(end-1,:),'*:')                % plot concentration against time

hold on

end

xlabel('Time(seconds)')                % label x-axis
ylabel('Velocity v(x,t) (m/s)')        % label y-axis
title('Effect of Area on Velocity ')    % title of 2D graph
grid                                    % insert grid lines to graph
legend('A=0.01','A=100','A=400','A=800',0)

```

The following values were obtain after running the program.

Table 1: Velocity versus time: Area =0.01,100,400,800

Time(secs)	Velocity(m/s/s)			
	A=0.01	A=100	A=400	A=800
0	0	0	0	0
0.05	0.0081	0.0081	0.0081	0.0081
0.1	0.0162	0.0162	0.0162	0.0162
0.15	0.0241	0.0243	0.0249	0.0257
0.2	0.032	0.0328	0.0359	0.0413
0.25	0.0398	0.042	0.0514	0.0709
0.3	0.0475	0.0521	0.0746	0.1251
0.35	0.0552	0.0636	0.1092	0.2172
0.4	0.0628	0.0769	0.1595	0.3627
0.45	0.0704	0.0924	0.2306	0.5786
0.5	0.0779	0.1106	0.3279	0.8831
0.55	0.0854	0.1322	0.4574	1.2946
0.6	0.0928	0.1577	0.6251	1.8307
0.65	0.1002	0.1877	0.8374	2.5079
0.7	0.1075	0.223	1.1007	3.3399
0.75	0.1149	0.2641	1.4212	4.337
0.8	0.1222	0.3119	1.8051	5.5053
0.85	0.1295	0.3671	2.2577	6.8453
0.9	0.1367	0.4305	2.7841	8.3515
0.95	0.144	0.503	3.3885	10.0118
1	0.1512	0.5854	4.074	11.8069

APPENDIX II: MATLAB codes of effect of lateral inflow length on velocity

```

% Numerical Study of Fluid Flow in an open rectangular Channel

% #####

% solve  $y_t + v*y_x + (A/T)v_x = (2q/TL)\sin(\theta)$   $0 \leq x \leq xf$ ,  $0 \leq t \leq t_{final}$ 

%  $v_t + v*v_x + gy_x + g(sf-s_0) = (2q/AL)\sin(\theta)(\cos(\theta) - v)$   $0 \leq x \leq xf$ ,  $0 \leq t \leq t_{final}$ 

% Initial Condition:  $y(x,0) = ity_0(x)$ 

%  $v(x,0) = itv_0(x)$ 

%

% Boundary Conditions:  $y(0,t) = g_0(t) = by_0(t)$  (left BC)

%  $y(xf,t) = g_1(t) = by_1(t)$  (right BC)

%  $v(0,t) = h_0(t) = bv_0(t)$  (left BC)

%  $v(xf,t) = h_1(t) = bv_1(t)$  (right BC)

clc,clf,clear all,close all% clear screen,clear figure,clear all declared variables, close all figures

A=1;

T=10; % Top width

q=0.3; % Discharge

theta=pi/3; % Angle of discharge

g=9.82; % gravitational force

s0=0.002;

n=0.01;R=1.1;

u=10;

t0=0; % initial time

x0=0; % initial distance

```

```

xfinal=100;      % maximum distance final distance/distance at which concentration is
to be calculated

tfinal=1;       % maximum time (final time)

M=5;           % M = # of subintervals along x(distance) axis

N=20;         % N = # of subintervals along t(time) axis

dx = (xfinal-x0)/M ; % distance interval

x = [0:M]*dx;   % values of distance (x)

dt = (tfinal-t0)/N; % time interval

t = [0:N]*dt;   % values of time (t)

% initial and boundary conditions formulae definitions(next three lines)
ity0=inline('0','x','t');itv0=inline('0','x','t');
by0=inline('30','x','t');bv0=inline('20','x','t');
byf=inline('10','x','t');bvf=inline('20','x','t');

for i = 1:M + 1,

    y(i,1) = ity0(x(i),t(1)); % initial condition evaluation
    v(i,1) = itv0(x(i),t(1)); % initial condition evaluation
end

for j = 1:N + 1

    y(1,j) = by0(x(1),t(j)); % boundary conditions evaluations
    y(M+1,j)=byf(x(M+1),t(j)); % boundary conditions evaluations
    v(1,j) = bv0(x(1),t(j)); % boundary conditions evaluations
    v(M+1,j)=bvf(x(M+1),t(j)); % boundary conditions evaluations
end

% if gt(dt/(2*dx),1) % stability condition: 2*D_L*dt/dx^2 <= 1

```

```

% error('stability condition not satisfied') % error message if stability condition is
not satisfied

% return % return control to command line

% end % end of stability condition loop

for L=[10 100 1000 10000]

for j = 1:N % start of time loop

for i = 2:M % start of distance loop

y(i,j+1)=dt*(-v(i,j).*((y(i+1,j)-y(i-1,j))/(2*dx))-(A/T)*((v(i+1,j)-v(i-
1,j))/(2*dx)))+(2*q/(T*L))*sin(theta))+y(i,j)

v(i,j+1)=dt*(-v(i,j).*((v(i+1,j)-v(i-1,j))/(2*dx))-g*((y(i+1,j)-y(i-1,j))/(2*dx))-
g*(n^2*(v(i,j).^2/R^(4/3))-s0)+(2*q/(T*L))*sin(theta)*(u*cos(theta)-v(i,j))))+v(i,j)

end % end of distance loop

end % end of time loop

plot(t,v(end-2,:),'*:') % plot concentration against time

hold on

end

xlabel('Time(seconds)') % label x-axis

ylabel('Velocity v(x,t) (m/s)') % label y-axis

title('Effect of Length on Velocity ') % title of 2D graph

grid % insert grid lines to graph

legend('L=10','L=100','L=1000','L=10000',0)

```

The following values were obtain after running the program.

Table 2: Velocity versus time:L=10,100,1000,10000

Time(secs)	Velocity(m/s/s)			
	L=10	L=100	L=1000	L=10000
0	0	0	0	0
0.05	0.0023	0.0011	0.001	0.001
0.1	0.0046	0.0023	0.002	0.002
0.15	0.0069	0.0034	0.0031	0.003
0.2	0.0092	0.0046	0.0041	0.004
0.25	0.0115	0.0057	0.0051	0.005
0.3	0.0138	0.0068	0.0061	0.006
0.35	0.016	0.0078	0.007	0.0069
0.4	0.0182	0.0088	0.0079	0.0078
0.45	0.0202	0.0097	0.0086	0.0085
0.5	0.0222	0.0105	0.0093	0.0092
0.55	0.0241	0.0111	0.0099	0.0097
0.6	0.0258	0.0117	0.0103	0.0101
0.65	0.0274	0.0121	0.0106	0.0104
0.7	0.0289	0.0124	0.0107	0.0105
0.75	0.0302	0.0124	0.0107	0.0105
0.8	0.0313	0.0123	0.0104	0.0103
0.85	0.0322	0.0121	0.01	0.0098
0.9	0.033	0.0116	0.0094	0.0092
0.95	0.0335	0.0109	0.0086	0.0084
1	0.0339	0.01	0.0076	0.0073

APPENDIX III: MATLAB codes of effect of angle on velocity

```

% Numerical Study of Fluid Flow in an open rectangular Channel

% #####

% solve  $y_t + v*y_x + (A/T)v_x = (2q/TL)\sin(\theta)$   $0 \leq x \leq xf$ ,  $0 \leq t \leq t_{final}$ 

%  $v_t + v*v_x + g*y_x + g(sf-s0) = (2q/AL)\sin(\theta)(\cos(\theta) - v)$   $0 \leq x \leq xf$ ,  $0 \leq t \leq t_{final}$ 

% Initial Condition:  $y(x,0) = ity0(x)$ 

%  $v(x,0) = itv0(x)$ 

%

% Boundary Conditions:  $y(0,t) = g0(t) = by0(t)$  (left BC)

%  $y(xf,t) = g1(t) = byf(t)$  (right BC)

%  $v(0,t) = h0(t) = bv0(t)$  (left BC)

%  $v(xf,t) = h1(t) = bv1(t)$  (right BC)

clc,clf,clear all,close all% clear screen,clear figure,clear all declared variables, close all figures

L=1;

A=1;

T=10; % Top width

q=0.3; % Discharge

g=9.82; % gravitational force

s0=0.002;

n=0.01;R=1.1;

u=10;

t0=0; % initial time

x0=0; % initial distance

```

```

xfinal=100;      % maximum distance final distance/distance at which concentration is
to be calculated

tfinal=1;       % maximum time (final time)

M=5;           % M = # of subintervals along x(distance) axis

N=20;          % N = # of subintervals along t(time) axis

dx = (xfinal-x0)/M ; % distance interval

x = [0:M]*dx;   % values of distance (x)

dt = (tfinal-t0)/N; % time interval

t = [0:N]*dt;   % values of time (t)

% initial and boundary conditions formulae definitions(next three lines)
ity0=inline('0','x','t');itv0=inline('0','x','t');
by0=inline('30','x','t');bv0=inline('20','x','t');
byf=inline('10','x','t');bvf=inline('20','x','t');

for i = 1:M + 1,

    y(i,1) = ity0(x(i),t(1)); % initial condition evaluation
    v(i,1) = itv0(x(i),t(1)); % initial condition evaluation
end

for j = 1:N + 1

    y(1,j) = by0(x(1),t(j)); % boundary conditions evaluations
    y(M+1,j)=byf(x(M+1),t(j)); % boundary conditions evaluations
    v(1,j) = bv0(x(1),t(j)); % boundary conditions evaluations
    v(M+1,j)=bvf(x(M+1),t(j)); % boundary conditions evaluations
end

% if gt(dt/(2*dx),1) % stability condition: 2*D_L*dt/dx^2 <= 1

```

```

% error('stability condition not satisfied') % error message if stability condition is
not satisfied

% return % return control to command line

% end % end of stability condition loop

for theta=[pi/4 pi/3 pi/2.5 pi/2]

for j = 1:N % start of time loop

for i = 2:M % start of distance loop

y(i,j+1)=dt*(-v(i,j).*((y(i+1,j)-y(i-1,j))/(2*dx))-(A/T)*((v(i+1,j)-v(i-
1,j))/(2*dx)))+(2*q/(T*L))*sin(theta))+y(i,j)

v(i,j+1)=dt*(-v(i,j).*((v(i+1,j)-v(i-1,j))/(2*dx))-g*((y(i+1,j)-y(i-1,j))/(2*dx))-
g*(n^2*(v(i,j).^2/R^(4/3))-s0)+(2*q/(T*L))*sin(theta)*(u*cos(theta)-v(i,j))))+v(i,j)

end % end of distance loop

end % end of time loop

plot(t,v(end-2,:),'*:') % plot concentration against time

hold on

end

xlabel('Time(seconds)') % label x-axis

ylabel('Velocity v(x,t) (m/s)') % label y-axis

title('Effect of Angle on Velocity ') % title of 2D graph

grid % insert grid lines to graph

legend('Angle=pi/4','Angle=pi/3','Angle=pi/2.5','Angle=pi/2',0)

```

The following values were obtained after running the program.

Table 3: Velocity versus time: Angle = $\pi/4, \pi/3, \pi/2.5, \pi/2$

Time(secs)	Velocity(m/s/s)			
	$\pi/4$	$\pi/3$	$\pi/2.5$	$\pi/2$
0	0	0	0	0
0.05	0.016	0.014	0.0098	0.001
0.1	0.032	0.0279	0.0196	0.002
0.15	0.0479	0.0419	0.0294	0.003
0.2	0.0639	0.0558	0.0392	0.004
0.25	0.0798	0.0697	0.0489	0.005
0.3	0.0957	0.0835	0.0586	0.006
0.35	0.1115	0.0973	0.0682	0.0069
0.4	0.1272	0.111	0.0778	0.0077
0.45	0.1429	0.1247	0.0872	0.0084
0.5	0.1585	0.1382	0.0966	0.009
0.55	0.1741	0.1517	0.1059	0.0096
0.6	0.1895	0.165	0.115	0.01
0.65	0.2048	0.1782	0.1241	0.0102
0.7	0.22	0.1913	0.133	0.0103
0.75	0.2351	0.2043	0.1417	0.0103
0.8	0.2501	0.2172	0.1503	0.01
0.85	0.265	0.2299	0.1588	0.0096
0.9	0.2797	0.2425	0.1671	0.009
0.95	0.2943	0.2549	0.1752	0.0082
1	0.3088	0.2672	0.1832	0.0072

